Geophysical Research Letters

RESEARCH LETTER
10.1029/2018GL079137

Key Points:
- A robust definition for identifying recurrence of sea surface temperature anomalies (SSTA) is proposed
- Most of the global ocean exhibits winter-to-winter recurrence of SSTA
- Recurrence of SSTA in the tropics is related to the recurrence of wind-stress forcing

Supporting Information:
- Supporting Information S1

Correspondence to:
P. Byju,
byju.pookkandy@monash.edu

Citation:
Byju, P., Dommenget, D., & Alexander, M. A. (2018). Widespread reemergence of sea surface temperature anomalies in the global oceans, including tropical regions forced by reemerging winds. *Geophysical Research Letters*, *45*, 7683–7691. https://doi.org/10.1029/2018GL079137

Received 8 JUN 2018
Accepted 18 JUL 2018
Accepted article online 25 JUL 2018
Published online 11 AUG 2018

Widespread Reemergence of Sea Surface Temperature Anomalies in the Global Oceans, Including Tropical Regions Forced by Reemerging Winds

P. Byju[1], D. Dommenget[1], and M. A. Alexander[2]

[1]School of Earth, Atmosphere and Environment, Monash University, Clayton, Victoria, Australia, [2]NOAA/ESRL, Boulder, CO, USA

Abstract Sea surface temperature anomalies (SSTA) in portions of the extratropics are known to recur from one winter to the next without persisting through the intervening summer. Previous studies identified only a limited number of midlatitude regions where this reemergence occurs. Here we find that most of the global oceans exhibit winter-to-winter recurrence of SSTA. Indeed, recurrence of SSTA is the default process in the global ocean. Only regions strongly linked to El Niño do not show signs of SST reemergence. In midlatitudes, the temperature anomalies that recur persist below the shallow mixed layer in summer. However, SST recurrence is also found at some tropical locations and appears to be independent of subsurface ocean heat storage. Reemergence at these locations is linked to the recurrence of atmospheric drivers of SSTA, predominantly the wind-stress forcing. Our results are supported by different ocean data sets and by state-of-the-art climate model simulations.

Plain Language Summary The study addresses the global distribution of the reemergence of sea surface temperature (SST) anomalies. The reemergence of SST is the phenomenon that SST anomalies from one winter to the next reemerge, while they apparently disappear in the summer. This is linked to the SST anomalies being stored in the subsurface ocean. Recent studies have shown the role of reemergence on European weather, North Atlantic Oscillations, and Pacific Decadal Oscillation. In this study we show the regions where this phenomenon is strong in the global ocean and different mechanism that cause the recurrence. Here we find that the recurrence of SST anomalies is also apparent in the tropics, which is linked to the recurrence of wind-stress forcing at the location.

1. Introduction

The large thermal inertia of the ocean enables the sea surface temperature (SST) anomalies (SSTA) to persist, which may influence the atmospheric circulation and weather conditions through air-sea interaction (Deser et al., 2003; Gastineau & Frankignoul, 2015). Previous studies have shown that the winter SSTA in some midlatitude locations has the tendency to recur in the following winter without persisting through the intervening summer (Namias & Born, 1970, 1974). This SSTA recurrence, also called the reemergence mechanism (Alexander & Deser, 1995), is associated with seasonally varying mixed layer depth (MLD; Alexander & Deser, 1995; Namias et al., 1988). During winter, temperature anomalies are homogeneously distributed over a deep mixed layer due to strong wind mixing and surface buoyancy forcing. During spring and summer, heating by the Sun strengthens the upper ocean stratification and the mixed layer shoals, which caps the ocean temperature anomalies created in winter below the surface in the summer seasonal thermocline. These thermal anomalies remain insulated from further dissipation by mechanical and thermodynamic ocean processes. When the mixed layer deepens in the fall and the following winter, part of these sequestered temperature anomalies is re-entrained into the mixed layer and interact with the concurrent SST.

The reemerging SSTAs are independent of the concurrent atmospheric heat fluxes and can recur for longer than 1 year due to the persistence of thermal anomalies in the subsurface ocean. A number of studies have documented winter SSTA recurrence in portions of the North Pacific (Alexander et al., 1999; Alexander & Deser, 1995; Deser et al., 2003; Namias & Born, 1970, 1974; Namias et al., 1988), North Atlantic (de Coëtlogon & Frankignoul, 2003; Kushnir et al., 2002; Timlin et al., 2002; Watanabe & Kimoto, 2000), and in the Southern Hemisphere (Ciasto & Thompson, 2009; Hadfield, 2000). All of these studies have found reemergence in the extratropical ocean basins and that the seasonal variation of MLD is the dominant mechanism behind this feature (Alexander & Deser, 1995; Namias et al., 1988). Studies also showed that ocean currents can remove the SSTA away from the location even before they could be entrained into the mixed layer and reemerge at another location (de Coëtlogon & Frankignoul, 2003; Sugimoto & Hanawa, 2005a, 2005b). Also, the remote El Niño-Southern Oscillation (ENSO) forcing can partly modulate entrainment processes and influence the amplitude of the recurring temperature anomalies (Deser et al., 2012; Park et al., 2006). Reemergence was found to occur in some parts of the midlatitude ocean, constituting ~17% of the global ocean, where these areas were characterized in terms of MLD, annual mean heat flux, and water mass formed in winter (Hanawa & Sugimoto, 2004). However, the criteria used by previous studies (the secondary maximum of lag correlation should exceed 99% significance level; e.g., Hanawa & Sugimoto, 2004) may have missed areas of reemergence, by not fully considering the decaying nature of the SST autocorrelation. Thus, we seek to identify where SSTA recurrence occurs and the processes driving it using ocean reanalysis data and Coupled Model Intercomparison Project (CMIP5) simulations.

2. Data and Methods

Monthly sea surface and subsurface temperatures were obtained from the German contribution to Estimating the Circulation and Climate of the Ocean System (GECCO2; Köhl, 2015) for the period 1948–2011. We used lag correlations, applied at each grid point, to detect the recurrence of SSTA and the net surface heat flux and wind stress over the global ocean. The initialization period for the autocorrelations was based on cold season, taken here to be January–February (August–September) in the Northern (Southern) Hemisphere. These months are in general the month when the climatological mixed layer is the deepest in most parts of the respective hemisphere. This even holds for most parts of the tropical regions. The winter-to-winter recurrence of SSTA is then identified by computing the difference between 12- and 6-month lag autocorrelation. The 6-month lag points to the peak summer months (corresponding to the choice of cold season) where the cold season (lag 0) SSTA exhibits a weak persistent correlation. We define this difference (12- and 6-month lag) as the reemergence index (RE index). The results for the RE index are not sensitive to shifting the lag by ±1 month. We used the same calendar months for computing the cold season autocorrelation difference of anomalies of net heat flux (NHFA) and wind stress (TAUA).

The warm season, used to compute the ratio of MLD (Figures 4a and 4d), was defined as July–August (December–January) in the Northern (Southern) Hemisphere. The MLD was computed using the shallowest extreme curvature criteria (Lorbacher et al., 2006) applied to the density profiles. We performed similar analyses using different ocean data sets including the National Centers for Environmental Prediction Global Ocean Data Assimilation System (NCEP-GODAS) for the period 1980–2013, the Simple Ocean Data Assimilation for the period 1950–2010 (Carton & Giese, 2008), and Hadley Centre's sea Ice and Sea Surface Temperature data from 1870 to 2011 (Rayner et al., 2003). The RE index computed, using these data sets (supporting information Figure S1), is consistent with the results from GECCO2, as are the recurrence values for NHFA and TAUA (Figure S2, including NCEP-National Center for Atmospheric Research [Kalnay et al., 1996] reanalysis for the period 1948–2014). However, differences are obvious between these data sets, which could be associated with different model assimilation procedures (Kröger et al., 2012).

We also used monthly data from preindustrial control simulations (in which greenhouse gases are fixed at 1,850 levels) in CMIP5 (Taylor et al., 2012). The CMIP5 project includes models from different institutions with different spatial and temporal resolution. We used 44 such models (Table 1), with control simulations that are at least 200 years long, and most are 500 years long. The RE index was computed from the individual models and then ensemble averaged to indicate the areas of SSTA recurrence in Figure 2c. MLD for each model was computed using the shallowest extreme curvature criteria (Lorbacher et al., 2006) applied to the density profiles. The ratio of MLD shown in Figure 2d is based on the 18 models that had salinity and temperature data available (marked "*" in Table 1). The same calendar months of cold and warm season as in GECCO2 have been used for computing the MLD ratio for CMIP5 analysis. The recurrence of NHFA and TAUA are based on 39 CMIP5 models (marked "^" in Table 1). We excluded remaining models from computing the ensemble of atmospheric forcing recurrence because either the data were not available or the data appear to have been corrupted in some way.

10.1029/2018GL079137

Table 1
List of Pi Control Coupled Model Intercomparison Project Models

Sr. no.	Models	Sr. no.	Models	Sr. no.	Models
1	ACCESS1.0^	16	CNRM-CM5–2^	31	IPSL-CM5A-LR^*
2	ACCESS1.3^*	17	CSIRO-Mk3–6-0^*	32	IPSL-CM5A-MR^
3	BNU-ESM^*	18	EC-EARTH	33	IPSL-CM5B-LR^
4	BCC-CSM1.1-m^	19	FGOALS-s2^	34	KCM1–2-2
5	BCC-CSM1.1^*	20	FGOALS-g2^*	35	MIROC-ESM-CHEM^
6	CanESM2^*	21	FIO-ESM	36	MIROC-ESM^
7	CCSM4^*	22	GISS-E2-H-CC^	37	MIROC4h^*
8	CESM1-WACCM^	23	GISS-E2-R-CC^	38	MIROC5^
9	CESM1-BGC^*	24	GISS-E2-R	39	MRI-CGCM3^*
10	CESM1-CAM5^*	25	GISS-E2-H^*	40	MPI-ESM-LR^
11	CESM1-FASTCHEM^	26	GFDL-CM3^*	41	MPI-ESM-MR^
12	CMCC-CM^	27	GFDL-ESM 2 M^*	42	MPI-ESM-P^
13	CMCC-CESM^*	28	GFDL-ESM 2G^	43	NorESM1-ME^
14	CMCC-CMS^	29	HadGEM2-CC^*	44	NorESM1-M^
15	CNRM-CM5^*	30	HadGEM2-AO		

Note. Models with "*" represent models that used to compute the mixed layer depth multimodel mean shown in Figure 2d (18 models) and with "^" are included to compute ensemble of anomalies of net heat flux and wind stress recurrence shown in Figures 4c and 4d (39 models).

3. Results and Discussions

The reemergence signal was detected based on the lag autocorrelation of SSTA starting in winter (Alexander et al., 1999, 2001; Alexander & Deser, 1995). We illustrate the lag autocorrelation of the upper ocean temperature with the SSTA in August (austral winter) at a reemergence location in the Southern Hemisphere (Figure 1a) and at a nonreemergence location in January (boreal winter) from the Northern Hemisphere (Figure 1b). At the reemergence location, the correlation from the winter SSTA decays slowly at depths greater than ~100 m, remaining high until the next winter. At the surface, the correlation decreases rapidly in spring but then increase in fall, indicative of the reemergence process, which is well illustrated by autocorrelations of SSTA with SSTAs in the previous winter (blue line; Figure 1c). In contrast, at the nonreemergence location, correlations to winter SSTA monotonically decrease at all depths including the surface.

The lag autocorrelation of SSTA in the absence of reemergence is expected to follow an exponential decay of the theoretical auto-regressive process of order 1 (red noise). The most characteristic signature of a reemergence winter SSTA autocorrelation in comparison to that of a nonreemergence location (red noise) is the difference between the 12- and the 6-month lag correlations (RE index). The expectation of the RE index is about -0.2 for a red noise process with the 1-month lag autocorrelation of $r = 0.77$, as in the average of all global SSTA (Figure 1d). The probability distribution of the RE index for a red noise process depends on the length of the time series of SSTA (Figure 1d). However, even for the relatively short observation period of 60 years for the GECCO2 data set, an RE value >0 is fairly unlikely (probability $<1\%$).

We now investigate the recurrence areas of winter SSTA in the world ocean based on the RE index using reanalysis data (GECCO2). Figure 2a shows the cold season SSTA lag correlation difference between 12- and 6-month lag (RE index). Note that all autocorrelations are based on winter base months in each hemisphere. It reveals that the winter-to-winter recurrence of SST anomalies is more widespread in the global ocean (reddish shades) than previously thought (Hanawa & Sugimoto, 2004). It is estimated that about 54% of the oceanic area (spanning 65°N–65°S and 0–360) exhibits an RE index >0.0. The signal is strongest in the higher latitudes of the Southern Ocean and North Atlantic, but it is present at all latitudes. In the tropics, in particular in the equatorial central and eastern Pacific, and in areas with strong ENSO teleconnections such as the tropical Indian and the Atlantic Ocean, a reemergence signal is weak or not present.

The existence and strength of the reemergence phenomenon is strongly linked to the difference between cold and warm season MLD (Alexander & Deser, 1995; Namias et al., 1988). Regions with strong reemergence are in general regions that have mixed layer deep in the cold season and shallow in the warm season (de Boyer Montégut et al., 2004; Pookkandy et al., 2016; e.g., Figure 1a), which effectively separates the

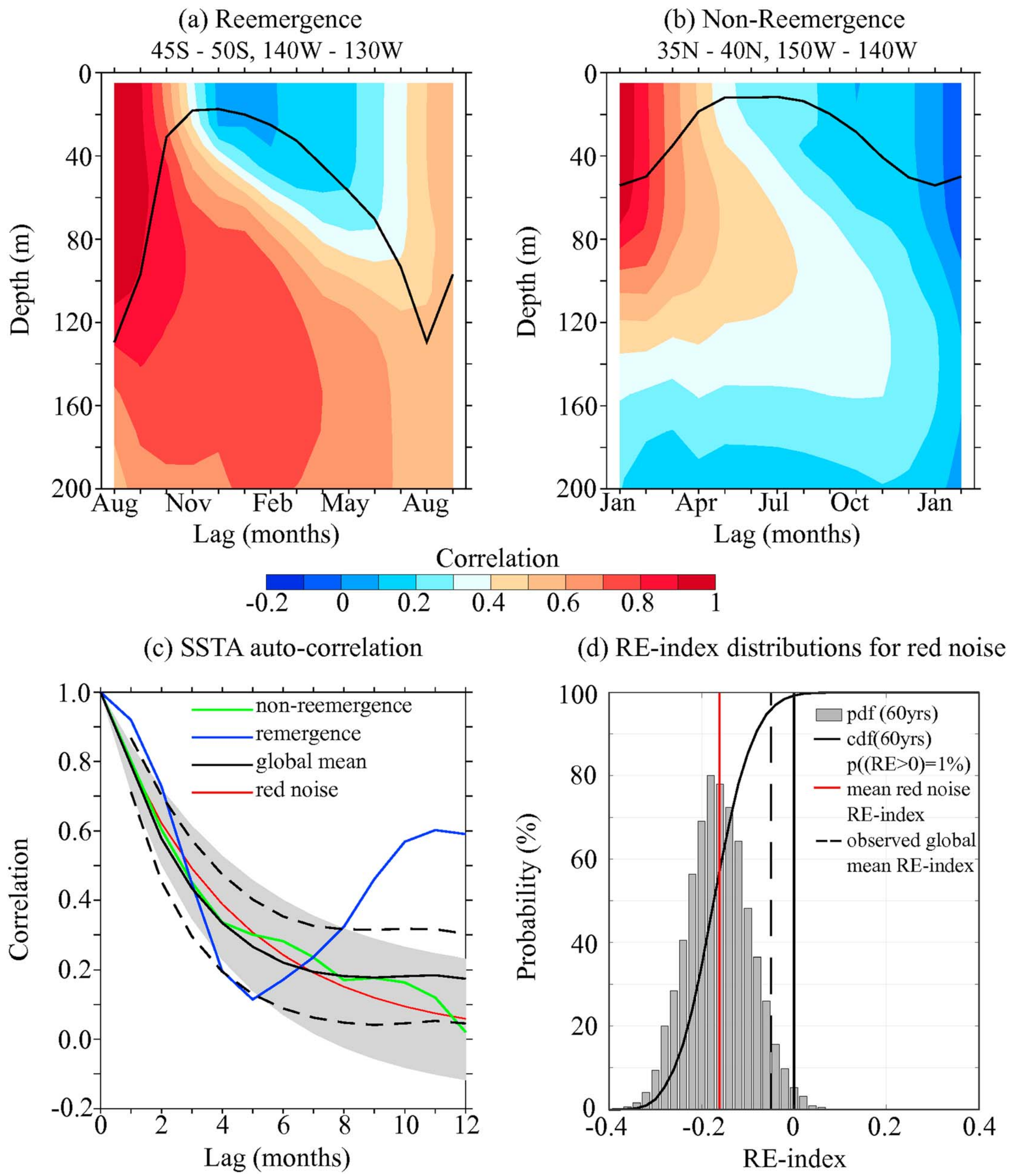

Figure 1. Distribution of lag correlation coefficients for winter SSTA to the temperature anomalies from the surface to 200-m depth at a location of (a) reemergence in the South Pacific Ocean and (b) nonreemergence in the North Pacific. Solid black line represents climatological mixed layer depth. (c) Autocorrelation of winter SST anomaly at a location showing reemergence (blue; location as in a) and nonreemergence (green; location as in b) from the German contribution to Estimating the Circulation and Climate of the Ocean System data set. The black line represents the global mean (average of 65S–65N and 0–360) SSTA autocorrelation over all seasons, and the dashed lines are ±1 standard deviation. The red line represents red noise auto-regressive process (order 1) and 95% significance shaded with gray. (d) Probability distribution of the RE index for a red noise process of a 60-year long time series with a lag-1 autocorrelation of 0.77, as in the average of the global SSTA. RE index = reemergence index; SSTA = sea surface temperature anomalies.

subsurface winter SSTA from the summer atmospheric forcing. Therefore, the ratio between cold and warm season MLD is a good indicator of where reemergence is favorable (Figure 2b). In general, the MLD ratio is large where the RE index is large; that is in the midlatitudes, particularly strong in the Indian and Pacific parts of the Southern Ocean and in the northern North Atlantic. However, there are a number of regions where significant differences can be noted. For instance, in the central to eastern North Pacific, the MLD

10.1029/2018GL079137

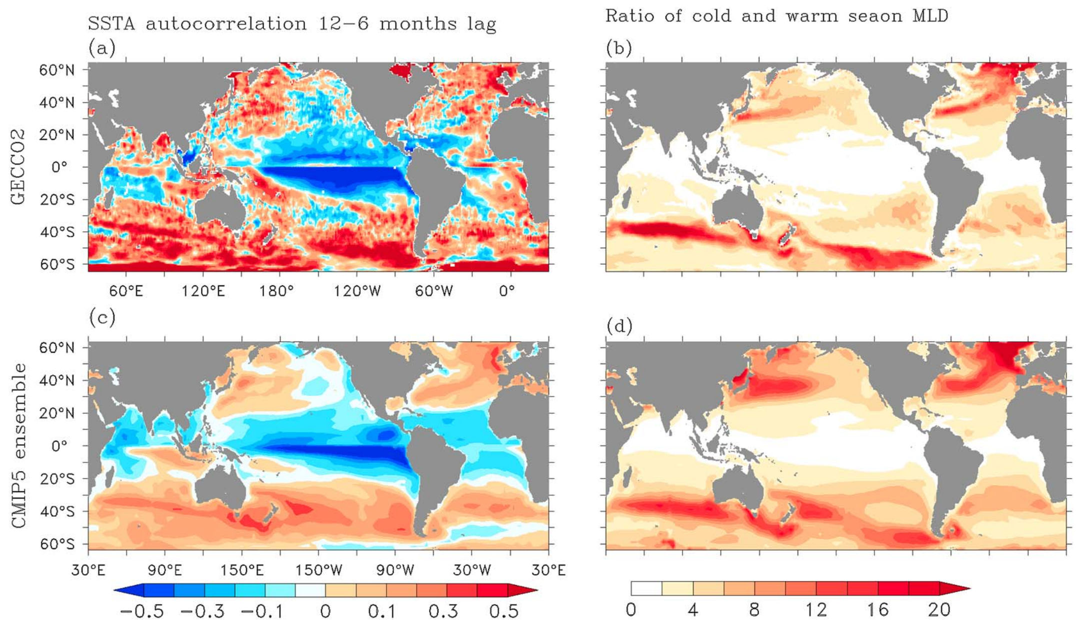

Figure 2. Spatial map of recurrence of SSTA (reemergence index) computed as the difference between 12- and 6-month lag autocorrelation based on winter base months in each hemisphere from (a) GECCO2 and (c) CMIP5 multimodel ensemble mean. The spatial map of the ratio of cold and warm season MLD are shown in (b) and (d). The cold season in the Northern Hemisphere was defined as January–February and the Southern Hemisphere cold season being August–September. CMIP5 = Coupled Model Intercomparison Project; GECCO2 = German contribution to Estimating the Circulation and Climate of the Ocean System; MLD = mixed layer depth; SSTA = sea surface temperature anomalies.

ratio is relatively large, but the RE index indicates that reemergence is not present. At ~40°S in the Atlantic, the MLD ratio is comparable to the central to eastern North Pacific, but the RE index is relatively large. The most notable mismatch can be seen in low latitudes, where the MLD ratio is very small, but the RE index is relatively large in some locations, especially northeast and northwest of Australia.

In addition to the GECCO2 ocean reanalysis, we computed the RE index for other observational data (NCEP-GODAS, Simple Ocean Data Assimilation ocean reanalysis, and Hadley Centre's sea Ice and Sea Surface Temperature; see Figure S1), which confirm the main findings. We can gain further insight into the reemergence mechanism by analyzing preindustrial simulations of coupled general circulation models from the CMIP5 database. Reemergence is a process that arises from internal climate variability, and the CMIP5 simulations should be able to reproduce these signals as in the observed. The CMIP5 simulations have the great advantage of providing long time series (>200 years) of ocean data with dynamically consistent fields without any measurement uncertainties. The global distribution of the RE index in the CMIP5 ensemble matches the observed very well (Figure 2c), not only the large-scale meridional structure with increased reemergence at higher latitudes but also the more detailed smaller structures. For instance, the band of increased RE index in the Southern Ocean from South Africa to south of New Zealand, an elevated RE index values of the northwest of Great Britain and the absence of reemergence in the northeast Pacific. Also, the CMIP5 models capture the small RE index at about 50°S. However, considerable mismatch also observed in the tropical Atlantic and north Indian Ocean. Overall, 47% of the oceans between 65°N and 65°S exhibit a RE index >0 in the CMIP5 ensemble, which is similar to the observed value. The areas of strong reemergence, however, are located in somewhat different locations in each model (not shown), which reduces the strength of the reemergence signals in the CMIP5 ensemble mean.

The CMIP5 simulations also reproduce the ratio of the cold to warm season MLD fairly well (see Figure 2d), including the representation of regional structures. For instance, the central to eastern North Pacific has a fairly large MLD ratio but a small RE index, suggesting no reemergence in this region, consistent with observations. At ~40°S in the Atlantic, the MLD ratio is comparable to the central to east North Pacific, but the RE index is relatively strong as is observed. Finally, the strong RE index in the tropical regions northeast and

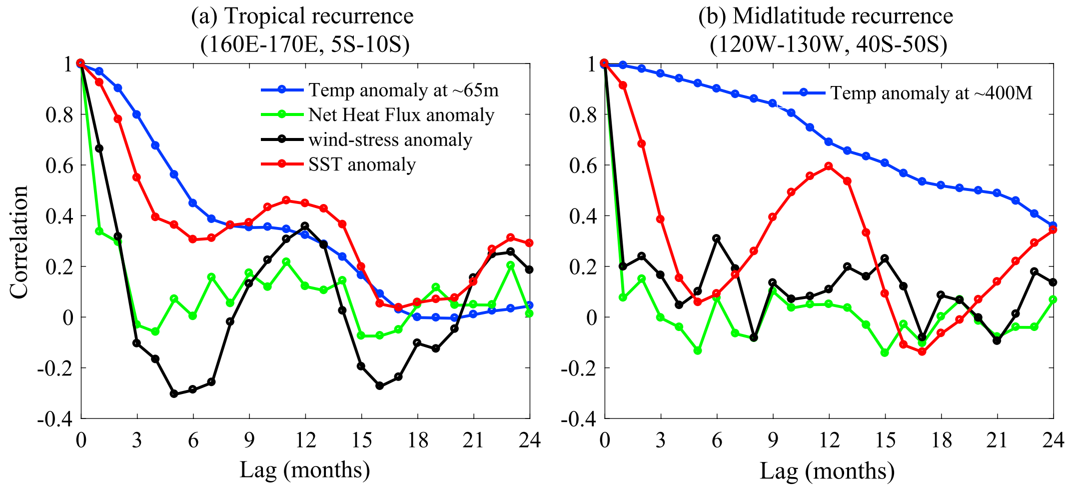

Figure 3. Lag correlation of winter time (here, August–September average) anomalies of temperature at surface and at depth corresponding to the bottom of the climatological winter mixed layer depth, net heat flux, and wind stress at a location in (a) the tropics and (b) midlatitude. The analysis is based from the German contribution to Estimating the Circulation and Climate of the Ocean System data set. SST = sea surface temperature.

northwest of Australia without large MLD ratios are also found in the CMIP simulations. It suggests that the tropical reemergence in the absence of strong seasonal MLD variability is not just a random fluctuation in the observations but is due to a real physical phenomenon.

To better understand the drivers of SSTA recurrence in these tropical locations, we analyzed the evolution of autocorrelation of anomalies of ocean temperature and atmospheric forcings at a recurring location in the Pacific Ocean (Figure 3a) and contrast it with a midlatitude location with strong reemergence (Figure 3b). The SSTA autocorrelation exhibits typical recurrence after 12-month lag in both the tropical and midlatitude locations. In the midlatitude location, the lag correlation of temperature anomalies at bottom of the climatological winter MLD (~400 m, blue curve, Figure 3b) exhibits strong persistence, and the SSTA autocorrelation at 12-month lag is slightly less than at depths below the winter MLD. It indicates that the persistent subsurface temperature anomalies are entrained to the upper ocean when the mixed layer deepens in the fall/winter, contributing to the concurrent SSTA. However, the temperature anomalies below the summer MLD in the tropical ocean (Figure 3a) do not persist, and the 12-month lag correlation of subsurface temperature anomalies is less than the SSTA correlation. This indicates the subsurface temperature anomalies are not significantly contributing to the recurrence of SSTA at the location via the classical reemergence mechanism. The evolution of autocorrelation anomalies in the tropical and midlatitude recurrence areas for CMIP5 simulations also reproduce fairly well (see Figure S5), including the SSTA showing a recurring pattern in the tropical location consistent with the recurrence of wind-stress anomalies.

We therefore analyzed the surface heat flux and wind-stress magnitude, the atmospheric variables that affect the thermal variability in the upper ocean. The atmospheric heat flux exhibits only a modest tendency to recur. However, wind-stress magnitude exhibits strong recurrence at 12-month intervals (Figure 3a), which coincides with the lag correlation curve of SSTA. It changes from modest negative correlations in summer to positive correlations in the following winter, suggesting that atmospheric wind-stress recurs from one winter to the next without persisting through the intervening summer. Such a signal is not present in the midlatitude location (Figure 3b).

In the tropical oceans, persistent and seasonally changing (recurring) atmospheric forcing is likely a key factor causing the recurrence of SSTA. The RE index for net heat flux and wind stress shows positive values in large areas of the global ocean (Figure 4). In general, the signal is noisier due to the low lag-1 autocorrelation of the atmospheric forcings, and the RE values have to be considered less significant than for the SSTA. However, the regions to the northeast and northwest of Australia do show indications (>95% significance level) of recurrence in the wind-stress forcing. The CMIP5 simulations support the aforementioned signature, but the strength of the recurring fluxes is stronger in observation than in the CMIP5 multimodel mean.

10.1029/2018GL079137

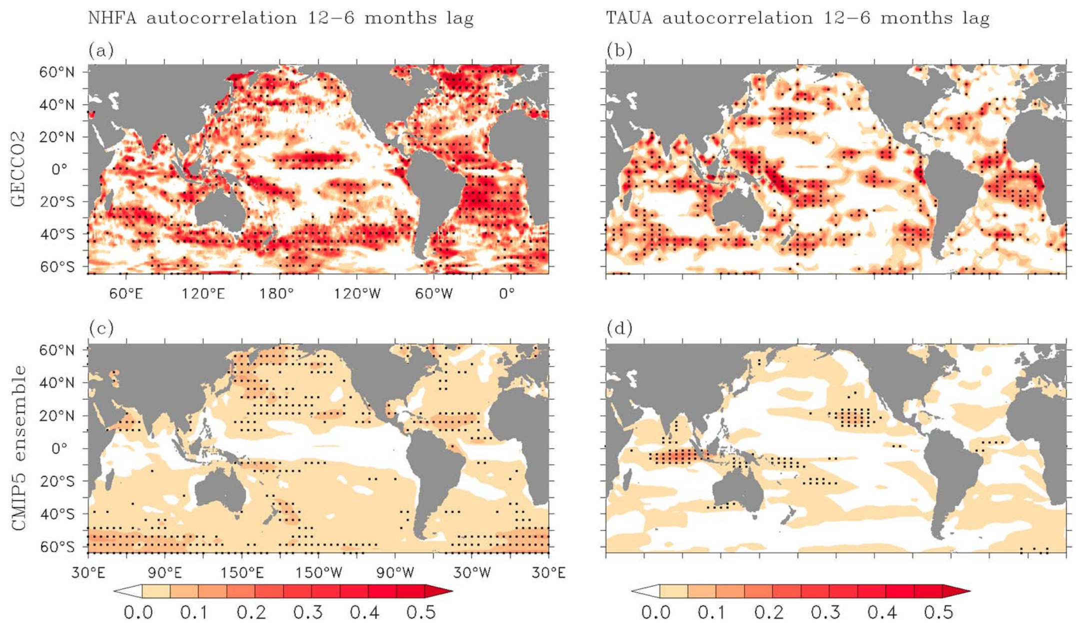

Figure 4. Spatial maps of recurrence (reemergence index) of net heat flux anomalies (a and c) and wind-stress anomalies (b and d) from GECCO2 (a and b) and CMIP5 ensemble (c and d) data, in respect to the winter months in each hemisphere. The dots indicate the reemergence index significant at the 95% confidence level. CMIP5 = Coupled Model Intercomparison Project; GECCO2 = German contribution to Estimating the Circulation and Climate of the Ocean System; NHFA = anomalies of net heat flux; TAUA = anomalies of wind stress.

However, the individual models show a better match to the observations (see Figures S3 and S4) again indicates that the signals are not just random fluctuations.

The regions of recurring atmospheric forcings coincide with the regions of SSTA recurrence in the tropics. The mismatch occurs in the central tropical Pacific, which is directly affected by ENSO, and does not show SSTA recurrence even in the presence of significant atmospheric recurrence in the observations. However, CMIP5 result shows the recurring SSTA only in the eastern tropical Indian and southwest Pacific that aligns with the significant wind-stress anomaly recurrence. Given that the atmosphere has a very short memory compared with thermal anomalies in the ocean, the cause of the recurrence in atmospheric fluxes is an open question. A potential source for the atmospheric recurrence in the forcings can be teleconnections associated with ocean-atmosphere coupled climate modes, such as ENSO (Bjerknes, 1969). Studies have also discovered winter-to-winter recurrence of atmospheric circulation and its influence on the reemergence of SSTA in the midlatitude North Pacific (Zhao & Li, 2010, 2012). The cause of this recurrence in atmospheric circulation is attributed to the seasonal variability of the storm track anomalies, which is not affected by major climate modes, such as ENSO and North Atlantic Oscillation.

Further, the winter-to-winter recurrence of SSTA is strongly influenced by the interannual and interdecadal variability of SSTA (Möller et al., 2008; Zhao & Li, 2010). A recent study (Sun et al., 2017) has found a prominent connection for multidecadal variability of wind and SST in the western tropical Pacific forced by the Atlantic Multidecadal Oscillation. Therefore, a recurrence of wind-stress and heat flux anomalies in the tropics (e.g., western tropical Pacific) could be modulated by the decadal climate variability. In further studies, we need to understand the recurrence of atmospheric forcing in other locations in detail, including its connection with modes of climate variability. Also, the relative contribution of atmospheric recurrence on SSTA reemergence, especially in the Southern Hemisphere, needs to be addressed.

4. Conclusions

In summary, the difference between 12- and 6-month lag correlations from SST anomalies in the previous winter indicates that winter-to-winter recurrence of SST anomalies is widespread in the global ocean. It can essentially be considered the default process in the global ocean. However, the regions that are strongly linked to ENSO (e.g., central-eastern tropical Pacific) do not show signs of SSTA recurrence. The mechanisms that generate winter-to-winter SSTA in the tropics and extra tropics can be substantially different. The seasonally varying MLD is the mechanism that predominates in midlatitudes (Alexander & Deser, 1995; Namias & Born, 1974), but recurring atmospheric forcing appears to be affecting SSTA recurrence in the tropics.

Both tropical and midlatitude SSTs can affect the atmospheric circulation, including those that recur in consecutive winters. For example, reemerging SSTAs in the North Atlantic have been shown to influence the North Atlantic Oscillation (Czaja & Frankignoul, 2002) and weather patterns over Europe (Cassou et al., 2007; Czaja & Frankignoul, 1999, 2002; Liu et al., 2007; Taws et al., 2011; Vannitsem, 2015). Thus, the recurrence of SSTA on annual time scales has the potential to enhance seasonal-to-interannual climate predictions.

Acknowledgments
The authors Pookkandy Byju and Dietmar Dommenget acknowledge the ARC Climate System Science (CE110001028) to support this study. The NCEP-GODAS data were provided by the NOAA/OAR/ESRL PSD, Boulder, Colorado, USA, from their website at http://www.esrl.noaa.gov/psd/. We acknowledge National Computational Infrastructure (NCI) in Canberra (Australia) for serving CMIP data for the study.

References

Alexander, M. A., Clara, D., & Timlin, M. (1999). The reemergence of SST anomalies in the North Pacific Ocean. *Journal of Climate*, *12*(8), 2419–2433. https://doi.org/10.1175/1520-0442(1999)012<2419:TROSAI>2.0.CO;2

Alexander, M. A., & Deser, C. (1995). A mechanism for the recurrence of wintertime midlatitude SST anomalies. *Journal of Physical Oceanography*, *25*(1), 122–137. https://doi.org/10.1175/1520-0485(1995)025<0122:AMFTRO>2.0.CO;2

Alexander, M. A., Timlin, M. S., & Scott, J. D. (2001). Winter-to-winter recurrence of sea surface temperature, salinity and mixed layer depth anomalies. *Progress in Oceanography*, *49*(1–4), 41–61. https://doi.org/10.1016/S0079-6611(01)00015-5

Bjerknes, J. (1969). Atmospheric teleconnections from the equatorial Pacific. *Monthly Weather Review*, *97*(3), 163–172. https://doi.org/10.1175/1520-0493(1969)097<0163:ATFTEP>2.3.CO;2

Carton, J. A., & Giese, B. S. (2008). A reanalysis of ocean climate using Simple Ocean Data Assimilation (SODA). *Monthly Weather Review*, *136*(8), 2999–3017. https://doi.org/10.1175/2007MWR1978.1

Cassou, C., Deser, C., & Alexander, M. A. (2007). Investigating the impact of reemerging sea surface temperature anomalies on the winter atmospheric circulation over the North Atlantic. *Journal of Climate*, *20*(14), 3510–3526. https://doi.org/10.1175/JCLI4202.1

Ciasto, L. M., & Thompson, D. W. J. (2009). Observational evidence of reemergence in the extratropical Southern Hemisphere. *Journal of Climate*, *22*(6), 1446–1453. https://doi.org/10.1175/2008JCLI2545.1

Czaja, A., & Frankignoul, C. (1999). Influence of the North Atlantic SST on the atmospheric circulation. *Geophysical Research Letters*, *26*, 2969–2972. https://doi.org/10.1029/1999GL900613

Czaja, A., & Frankignoul, C. (2002). Observed impact of Atlantic SST anomalies on the North Atlantic Oscillation. *Journal of Climate*, *15*(6), 606–623. https://doi.org/10.1175/1520-0442(2002)015<0606:OIOASA>2.0.CO;2

de Boyer Montégut, C., Madec, G., Fischer, A., Lazar, A., & Iudicone, D. (2004). Mixed layer depth over the global ocean: An examination of profile data and a profile-based climatology. *Journal of Geophysical Research*, *109*, C12003. https://doi.org/10.1029/2004JC002378

de Coëtlogon, G., & Frankignoul, C. (2003). The persistence of winter sea surface temperature in the North Atlantic. *Journal of Climate*, *16*(9), 1364–1377. https://doi.org/10.1175/1520-0442-16.9.1364

Deser, C., Alexander, M. A., & Timlin, M. S. (2003). Understanding the persistence of sea surface temperature anomalies in midlatitudes. *Journal of Climate*, *16*(1), 57–72. https://doi.org/10.1175/1520-0442(2003)016<0057:UTPOSS>2.0.CO;2

Deser, C., Phillips, A. S., Tomas, R. A., Okumura, Y. M., Alexander, M. A., Capotondi, A., et al. (2012). ENSO and Pacific decadal variability in the Community Climate System Model Version 4. *Journal of Climate*, *25*(8), 2622–2651. https://doi.org/10.1175/JCLI-D-11-00301.1

Gastineau, G., & Frankignoul, C. (2015). Influence of the North Atlantic SST variability on the atmospheric circulation during the twentieth century. *Journal of Climate*, *28*(4), 1396–1416. https://doi.org/10.1175/JCLI-D-14-00424.1

Hadfield, M. G. (2000). Atmospheric effects on upper-ocean temperature in the Southeast Tasman Sea. *Journal of Physical Oceanography*, *30*(12), 3239–3248. https://doi.org/10.1175/1520-0485(2000)030<3239:NACEOU>2.0.CO;2

Hanawa, K., & Sugimoto, S. (2004). 'Reemergence' areas of winter sea surface temperature anomalies in the world's oceans. *Geophysical Research Letters*, *31*, L10303. https://doi.org/10.1029/2004GL019904

Kalnay, E., Kanamitsu, M., & Kistler, R. (1996). The NCEP/NCAR 40-year reanalysis project. *Bulletin of the American Meteorological Society*, *77*(3), 437–471. https://doi.org/10.1175/1520-0477(1996)077<0437:TNYRP>2.0.CO;2

Köhl, A. (2015). Evaluation of the GECCO2 ocean synthesis: Transports of volume, heat and freshwater in the Atlantic: Evaluation of the GECCO2 ocean synthesis. *Quarterly Journal of the Royal Meteorological Society*, *141*(686), 166–181. https://doi.org/10.1002/qj.2347

Kröger, J., Müller, W. A., & von Storch, J.-S. (2012). Impact of different ocean reanalyses on decadal climate prediction. *Climate Dynamics*, *39*(3–4), 795–810. https://doi.org/10.1007/s00382-012-1310-7

Kushnir, Y., Robinson, W., Bladé, I., Hall, N., Peng, S., & Sutton, R. (2002). Atmospheric GCM response to extratropical SST anomalies: Synthesis and evaluation. *Journal of Climate*, *15*(16), 2233–2256. https://doi.org/10.1175/1520-0442(2002)015<2233:AGRTES>2.0.CO;2

Liu, Z., Liu, Y., Wu, L., & Jacob, R. (2007). Seasonal and long-term atmospheric responses to reemerging North Pacific Ocean variability: A combined dynamical and statistical assessment*. *Journal of Climate*, *20*(6), 955–980. https://doi.org/10.1175/JCLI4041.1

Lorbacher, K., Dommenget, D., Niiler, P. P., & Köhl, A. (2006). Ocean mixed layer depth: A subsurface proxy of ocean-atmosphere variability. *Journal of Geophysical Research*, *111*, C07010. https://doi.org/10.1029/2003JC002157

Möller, J., Dommenget, D., & Semenov, V. A. (2008). The annual peak in the SST anomaly spectrum. *Journal of Climate*, *21*(12), 2810–2823. https://doi.org/10.1175/2007JCLI2025.1

Namias, J., & Born, R. M. (1970). Temporal coherence in North Pacific Sea-surface temperature patterns. *Journal of Geophysical Research*, *75*, 5952–5955. https://doi.org/10.1029/JC075i030p05952

Namias, J., & Born, R. M. (1974). Further studies of temporal coherence in North Pacific Sea surface temperatures. *Journal of Geophysical Research*, *79*, 797–798. https://doi.org/10.1029/JC079i006p00797

Namias, J., Yuan, X., & Cayan, D. R. (1988). Persistence of North Pacific Sea surface temperature and atmospheric flow patterns. *Journal of Climate*, *1*(7), 682–703. https://doi.org/10.1175/1520-0442(1988)001<0682:PONPSS>2.0.CO;2

Park, S., Alexander, M. A., & Deser, C. (2006). The impact of cloud radiative feedback, remote ENSO forcing, and entrainment on the persistence of North Pacific Sea surface temperature anomalies. *Journal of Climate*, *19*(23), 6243–6261. https://doi.org/10.1175/JCLI3957.1

Pookkandy, B., Dommenget, D., Klingaman, N., Wales, S., Chung, C., Frauen, C., & Wolff, H. (2016). The role of local atmospheric forcing on the modulation of the ocean mixed layer depth in reanalyses and a coupled single column ocean model. *Climate Dynamics*, *47*(9–10), 2991–3010. https://doi.org/10.1007/s00382-016-3009-7

Rayner, N. A., Parker, D., Horton, E., Folland, C., Alexander, L., Rowell, D., et al. (2003). Global analyses of sea surface temperature, sea ice, and night marine air temperature since the late nineteenth century. *Journal of Geophysical Research*, *108*(D14), 4407. https://doi.org/10.1029/2002JD002670

Sugimoto, S., & Hanawa, K. (2005a). Remote reemergence areas of winter sea surface temperature anomalies in the North Pacific. *Geophysical Research Letters*, *32*, L01606. https://doi.org/10.1029/2004GL021410

Sugimoto, S., & Hanawa, K. (2005b). Why does reemergence of winter sea surface temperature anomalies not occur in eastern mode water areas? *Geophysical Research Letters*, *32*, L15608. https://doi.org/10.1029/2005GL022968

Sun, C., Kucharski, F., Li, J., Jin, F.-F., Kang, I.-S., & Ding, R. (2017). Western tropical Pacific multidecadal variability forced by the Atlantic multidecadal oscillation. *Nature Communications*, *8*, 15998. https://doi.org/10.1038/ncomms15998

Taws, S. L., Marsh, R., Wells, N. C., & Hirschi, J. (2011). Re-emerging ocean temperature anomalies in late-2010 associated with a repeat negative NAO. *Geophysical Research Letters*, *38*, L20601. https://doi.org/10.1029/2011GL048978

Taylor, K. E., Stouffer, R. J., & Meehl, G. A. (2012). An overview of CMIP5 and the experiment design. *Bulletin of the American Meteorological Society*, *93*(4), 485–498. https://doi.org/10.1175/BAMS-D-11-00094.1

Timlin, M. S., Alexander, M. A., & Deser, C. (2002). On the reemergence of North Atlantic SST anomalies. *Journal of Climate*, *15*(18), 2707–2712. https://doi.org/10.1175/1520-0442(2002)015<2707:OTRONA>2.0.CO;2

Vannitsem, S. (2015). The role of the ocean mixed layer on the development of the North Atlantic Oscillation: A dynamical system's perspective. *Geophysical Research Letters*, *42*, 8615–8623. https://doi.org/10.1002/2015GL065974

Watanabe, M., & Kimoto, M. (2000). On the persistence of decadal SST anomalies in the North Atlantic. *Journal of Climate*, *13*(16), 3017–3028. https://doi.org/10.1175/1520-0442(2000)013<3017:OTPODS>2.0.CO;2

Zhao, X., & Li, J. (2010). Winter-to-winter recurrence of sea surface temperature anomalies in the Northern Hemisphere. *Journal of Climate*, *23*(14), 3835–3854. https://doi.org/10.1175/2009JCLI2583.1

Zhao, X., & Li, J. (2012). Winter-to-winter recurrence of atmospheric circulation anomalies in the central North Pacific. *Journal of Geophysical Research*, *117*, C12023. https://doi.org/10.1029/2012JC008248